INTERNATIONAL JOURNAL FOR NUMERICAL METHODS IN ENGINEERING
Int. J. Numer. Meth. Engng 2000; **00**:1–6 *Prepared using* nmeauth.cls *[Version: 2002/09/18 v2.02]*

A domain decomposition method for discontinuous Galerkin discretizations of Helmholtz problems with plane waves and Lagrange multipliers

Charbel Farhat[‡], Radek Tezaur[‡] and Jari Toivanen[*,‡]

Department of Aeronautics and Astronautics, Department of Mechanical Engineering, and Institute for Computational and Mathematical Engineering, Stanford University, Mail Code 4035, Stanford, CA 94305, U.S.A.

SUMMARY

A nonoverlapping domain decomposition method is proposed for the iterative solution of systems of equations arising from the discretization of Helmholtz problems by the discontinuous enrichment method. This discretization method is a discontinuous Galerkin finite element method with plane wave basis functions for approximating locally the solution, and dual Lagrange multipliers for weakly enforcing its continuity over the element interfaces. The primal subdomain degrees of freedom are eliminated by local static condensations to obtain an algebraic system of equations formulated in terms of the interface Lagrange multipliers only. As in the FETI-H and FETI-DPH domain decomposition methods for continuous Galerkin discretizations, this system of Lagrange multipliers is iteratively solved by a Krylov method equipped with both a local preconditioner based on subdomain data, and a global one using a coarse space. Numerical experiments performed for two- and three-dimensional acoustic scattering problems suggest that the proposed domain decomposition based iterative solver is scalable with respect to both the size of the global problem and the number of subdomains.

KEY WORDS: discontinuous enrichment method; discontinuous Galerkin method; domain decomposition; GMRES; Lagrange multipliers; plane wave basis; preconditioning

1. INTRODUCTION

The oscillatory behavior of the solution of scattering problems in the medium and high frequency regimes is such that a fine discretization of the governing partial differential equation

[‡]E-mail: cfarhat@stanford.edu (C. Farhat), rtezaur@stanford.edu (R. Tezaur), toivanen@stanford.edu (J. Toivanen)
[*]Correspondence to: Jari Toivanen, Institute for Computational and Mathematical Engineering, Stanford University, Mail Code 4035, Stanford, CA 94305, U.S.A.

Contract/grant sponsor: U.S. Office of Naval Research; contract/grant number: N00014-08-1-0184

Contract/grant sponsor: Academy of Finland; contract/grant number: 207089

Received
Revised

(PDE) — usually, the Helmholtz equation — is required when the numerical approximation is based on polynomial functions. For this reason, plane wave based discretizations have become more popular for these problems during the last decade. For example, the partition of unity method [20], the ultra weak variational formulation [4, 18], a least-squares method [21], and the discontinuous enrichment/Galerkin method [8, 9] can employ plane waves. These approximation methods require fewer unknowns to reach a given accuracy when compared to finite element methods with polynomial basis functions. In this paper, attention is focused on the discontinuous enrichment method (DEM) [9, 13, 22, 25, 23] because of its established success for scattering problems in the medium frequency regime. DEM is a hybrid, discontinuous, multiscale method which enriches a continuous polynomial approximation at the element level with homogeneous solutions of the PDE to be solved. Hence for the Helmholtz equation, the element level enrichment consists of plane waves. Because such local enrichment is discontinuous in nature, DEM enforces a weak form of inter-element continuity and uses Lagrange multipliers for this purpose. For some wave propagation problems, the polynomial part of the approximation can be dropped, thereby transforming DEM into a non-standard discontinuous Galerkin method (DGM).

In the medium and high frequency regimes, the discretization of the Helmholtz equation leads to very large indefinite systems of linear equations that are difficult to solve efficiently. For traditional finite element discretizations, various iterative techniques have been proposed for the solution of such systems, including domain decomposition (DD) methods [7, 10, 11, 15, 19, 24], fictitious domain methods [16, 17], and multigrid methods [1, 2, 5, 6]. In the case of DEM, the algebraic system of equations turns out to be very ill-conditioned and therefore quite challenging for standard iterative solvers. For this reason, DEM has been equipped so far only with sparse direct solvers [13, 22, 25, 23]. In practice, this has placed an upper limit on the frequency that can be considered. To enable the solution of higher frequency problems, an iterative solution method has been developed for the DGM variant of DEM and is described in this paper.

Part of the proposed DD method is the static condensation of the enrichment variables and the elimination of the interior Lagrange multipliers. These two steps lead to an indefinite system of equations governing the Lagrange multipliers located at the subdomain interfaces. This system is solved here by the GMRES method equipped with two complementary preconditioners. The first one is an additive preconditioner based on subdomain problems. The second preconditioner is based on a projection onto the complement of a coarse space that is constructed using products of Lagrange basis functions and plane waves on each edge/face between the subdomains. The resulting DD based iterative solver resembles in some aspects the FETI-H method [10, 11] for continuous Galerkin discretizations.

The remainder of this paper is organized as follows. Section 2 begins with an overview of the discontinuous enrichment method for Helmholtz problems, its underlying hybrid variational formulation, and the corresponding discretization by plane wave basis functions and Lagrange multipliers. Then, this section follows with a presentation of the corresponding DD formulation and its regularization. Section 3 describes the transformation of the original problem into an interface problem with Lagrange multiplier unknowns, and introduces a local preconditioner and a coarse space projection to accelerate the solution of this problem by the GMRES method. Section 4 reports on performance results obtained for the solution of two- and three-dimensional acoustic scattering problems using DGM and its proposed DD based iterative solver, and compares these to the performance results obtained for the solution of the same problems

using standard finite element discretizations and the FETI-DPH method. Finally, Section 5 concludes this paper.

2. THE DISCONTINUOUS ENRICHMENT METHOD FOR HELMHOLTZ PROBLEMS

2.1. Hybrid variational formulation

The following exterior Helmholtz problem truncated in a domain Ω in $\mathbb{R}^n$, $n = 2, 3$, is considered: Find $u \in H^1(\Omega)$ such that

$$\begin{aligned} -\Delta u - k^2 u &= 0 && \text{in } \Omega \\ \frac{\partial}{\partial \boldsymbol{\nu}} u &= -\frac{\partial}{\partial \boldsymbol{\nu}} g && \text{on } \Sigma_1 \\ \frac{\partial u}{\partial \boldsymbol{\nu}} &= M(u) && \text{on } \Sigma_2, \end{aligned} \tag{1}$$

where k is the wavenumber, Σ_1 is the boundary of a sound-hard scatterer, and Σ_2 is the far-field boundary. The operator M defines an absorbing boundary condition and $\boldsymbol{\nu}$ denotes the unit outward normal. The function g specifies the incident field.

The computational domain Ω is partitioned into elements Ω_e in such a way that

$$\bar{\Omega} = \bigcup_{e=1}^{n_e} \bar{\Omega}_e \qquad \text{and} \qquad \bigcap_{e=1}^{n_e} \Omega_e = \emptyset. \tag{2}$$

In discontinuous Galerkin methods, the continuity of the solution across the element interfaces is not built into the finite element spaces. It can be enforced however in a weaker form by either penalizing the discontinuities or using Lagrange multipliers. In DEM and its DGM variant [8, 22, 25, 23], the latter approach is adopted. Hence, a space $\mathcal{V}$ for the primal variable u and a space $\mathcal{W}$ for the Lagrange multiplier λ are introduced as follows

$$\mathcal{V} = \left\{ v \in L^2(\widetilde{\Omega}) \ : \ v|_{\Omega_e} \in H^1(\Omega_e) \right\} \qquad \text{and} \qquad \mathcal{W} = \prod_{e=1}^{n_e} \prod_{e'=1}^{e-1} H^{-1/2}(\Gamma_{e,e'}), \tag{3}$$

where

$$\widetilde{\Omega} = \bigcup_{e=1}^{n_e} \Omega_e \qquad \text{and} \qquad \Gamma_{e,e'} = \partial\Omega_e \cap \partial\Omega_{e'}, \tag{4}$$

and problem (1) is transformed into the following hybrid variational problem:

Find $(u, \lambda) \in \mathcal{V} \times \mathcal{W}$ such that

$$\begin{aligned} a(u, v) + b(\lambda, v) &= r(v) && \forall v \in \mathcal{V} \\ b(\mu, u) &= 0 && \forall \mu \in \mathcal{W}, \end{aligned} \tag{5}$$

where the bilinear forms a on $\mathcal{V} \times \mathcal{V}$ and b on $\mathcal{W} \times \mathcal{V}$ are defined as

$$a(u, v) = \int_{\widetilde{\Omega}} (\nabla u \cdot \nabla v - k^2 u v) d\Omega - \int_{\Sigma_2} M(u) v d\Gamma \tag{6}$$

and

$$b(\lambda, v) = \sum_{e=1}^{n_e} \sum_{e'=1}^{e-1} \int_{\Gamma_{e,e'}} \lambda \left(v|_{\Omega_{e'}} - v|_{\Omega_e} \right) d\Gamma, \tag{7}$$

and the linear form r on $\mathcal{V}$ is defined as

$$r(v) = -\beta \int_{\Sigma_1} \frac{\partial g}{\partial \boldsymbol{\nu}} \, v \, d\Gamma. \tag{8}$$

2.2. Discretization

The discrete approximation of the space $\mathcal{V}$ is chosen to be spanned by solutions of the homogeneous Helmholtz equation. A natural set of such solutions is given by plane waves traveling in different directions. Thus, the space $\mathcal{V}$ is discretized by the subspace

$$\mathcal{V}_{n_\theta} = \left\{ u \in \mathcal{V} \ : \ u(\mathbf{x}) = \sum_{p=1}^{n_\theta} e^{ik\boldsymbol{\theta}_p^T \mathbf{x}} u_{e,p}, \ \ \mathbf{x} \in \Omega_e, \ \ u_{e,p} \in \mathbb{C} \right\}, \tag{9}$$

where $\boldsymbol{\theta}_p$, $p = 1, \ldots, n_\theta$, are unit wave propagation directions to be specified. The functions in $\mathcal{V}_{n_\theta}$ are solutions of the homogeneous Helmholtz equation in the interior of each element. Consequently, the volume integral in the bilinear form a can be reduced to integrals over element edges/faces using Green's formula. As a result, the matrices resulting from the volume integral can be computed more efficiently. For the two-dimensional and three-dimensional cases, this has been developed in [14] and [22], respectively.

For two-dimensional problems, the directions are uniformly distributed as follows

$$\boldsymbol{\theta}_p = \begin{pmatrix} \cos(2\pi(p-1)/n_\theta) \\ \sin(2\pi(p-1)/n_\theta) \end{pmatrix}, \quad p = 1, \ldots, n_\theta. \tag{10}$$

For three-dimensional problems, the following algorithm proposed in [22] can be used to generate the wave propagation directions

$$\mathbf{y}_{j_1,j_2,j_3} = \hat{\mathbf{y}}_{j_1,j_2,j_3} / \|\hat{\mathbf{y}}_{j_1,j_2,j_3}\|, \qquad \hat{\mathbf{y}}_{j_1,j_2,j_3} = \begin{pmatrix} \tan((2j_1/n_t - 1)\pi/4) \\ \tan((2j_2/n_t - 1)\pi/4) \\ \tan((2j_3/n_t - 1)\pi/4) \end{pmatrix}, \tag{11}$$

where n_t is a given positive integer, and $j_1, j_2, j_3 = 0, \ldots, n_t$ are positive integers chosen so that at least one of j_1, j_2, or j_3 is equal to zero or to n_t. Using this construction algorithm, the number of directions n_θ becomes equal to $6n_t^2 + 2$. For example, choosing $n_t = 2$, $n_t = 3$, and $n_t = 4$ leads to 26, 56, and 98 plane waves, respectively.

The discretization of the space of Lagrange multipliers $\mathcal{W}$ is a more delicate issue. The Lagrange multipliers are related to the normal derivatives of the primal variable at the element interfaces (for example, see [9]). Thus, one guideline for constructing the discretization of $\mathcal{W}$ is to approximate the normal derivative of u in the subspace spanned by the normal derivatives of the approximation of u in $\mathcal{V}_{n_\theta}$. However, this approximation cannot be too rich as it would violate the *inf-sup* condition guaranteeing the well-posedness of the discrete problem [3]. Hence, $\mathcal{W}$ is discretized by the subspace

$$\mathcal{W}_{n_\lambda} = \left\{ \lambda \in \mathcal{W} \ : \ \lambda(\mathbf{x}) = \sum_{p=1}^{n_\lambda} e^{ikc_p \boldsymbol{\phi}_p^T \boldsymbol{\tau}_{e,e'}(\mathbf{x})} \lambda_{e,e',p}, \ \ \mathbf{x} \in \Gamma_{e,e'}, \ \ \lambda_{e,e',p} \in \mathbb{C} \right\}, \tag{12}$$

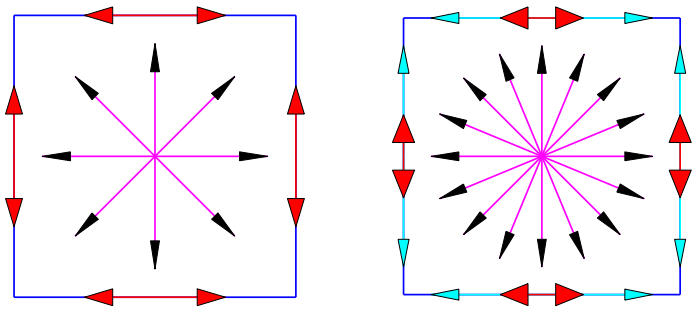

Figure 1. The quadrilateral elements Q-8-2 (left) and Q-16-4 (right) for two-dimensional problems. The vectors in the interior give the directions $\boldsymbol{\theta}_p$ and the vectors on the edges describe the coefficients c_p.

where the superscript T designates the transpose, c_p are given coefficients, $\boldsymbol{\phi}_p$ are unitary directions in $\mathbb{R}^{n-1}$, and $\boldsymbol{\tau}_{e,e'}(\mathbf{x})$ is the projection of $\mathbf{x}$ on local (orthogonal) coordinate(s) on the edge/face $\Gamma_{e,e'}$, and n_λ is the number of Lagrange multiplier degrees of freedom on each edge/face. Thus, $\mathcal{W}_{n_\lambda}$ too consists of waves propagating along the edges/faces of the elements. The richness of this subspace is controlled by the number of waves n_λ on each edge/face.

For two-dimensional problems, a quadrilateral element with n_θ directions for the primal variable and n_λ directions for the Lagrange multiplier is denoted by Q-n_θ-n_λ. The Q-8-2 and Q-16-4 elements shown in Figure 1 were introduced in [9, 13]. They have good approximation and stability properties. These elements are defined by $\boldsymbol{\phi}_p = 1$ in (12) where the c_p coefficients are set to

$$\{\pm 0.5\} \qquad \text{and} \qquad \{\pm 0.2, \pm 0.75\} \tag{13}$$

for the Q-8-2 and Q-16-4 elements, respectively.

For three-dimensional problems, an hexahedral element with n_θ directions for the primal variable and n_λ directions for the Lagrange multiplier is denoted by H-n_θ-n_λ. The H-26-4 and H-56-8 elements shown in Figure 2 were considered in [22], where it was demonstrated that these elements are at least one order of magnitude more accurate than polynomial finite elements of the same order of convergence. For the H-26-4 element, $c_p = 0.6$ for $p = 1, \ldots, 4$, and the directions are

$$\boldsymbol{\phi}_1 = \begin{pmatrix} \frac{1}{\sqrt{2}} \\ \frac{1}{\sqrt{2}} \end{pmatrix}, \quad \boldsymbol{\phi}_2 = \begin{pmatrix} \frac{1}{\sqrt{2}} \\ -\frac{1}{\sqrt{2}} \end{pmatrix}, \quad \boldsymbol{\phi}_3 = \begin{pmatrix} -\frac{1}{\sqrt{2}} \\ -\frac{1}{\sqrt{2}} \end{pmatrix}, \quad \boldsymbol{\phi}_4 = \begin{pmatrix} -\frac{1}{\sqrt{2}} \\ \frac{1}{\sqrt{2}} \end{pmatrix}. \tag{14}$$

The H-56-8 element is defined by setting $c_p = 0.8$ for $p = 1, \ldots, 4$, and choosing the corresponding directions to be the same as in (14), and setting $c_p = 0.5$ for $p = 5, \ldots, 8$ and choosing the corresponding directions as follows

$$\boldsymbol{\phi}_5 = \begin{pmatrix} 1 \\ 0 \end{pmatrix}, \quad \boldsymbol{\phi}_6 = \begin{pmatrix} 0 \\ 1 \end{pmatrix}, \quad \boldsymbol{\phi}_7 = \begin{pmatrix} -1 \\ 0 \end{pmatrix}, \quad \boldsymbol{\phi}_8 = \begin{pmatrix} 0 \\ -1 \end{pmatrix}.$$

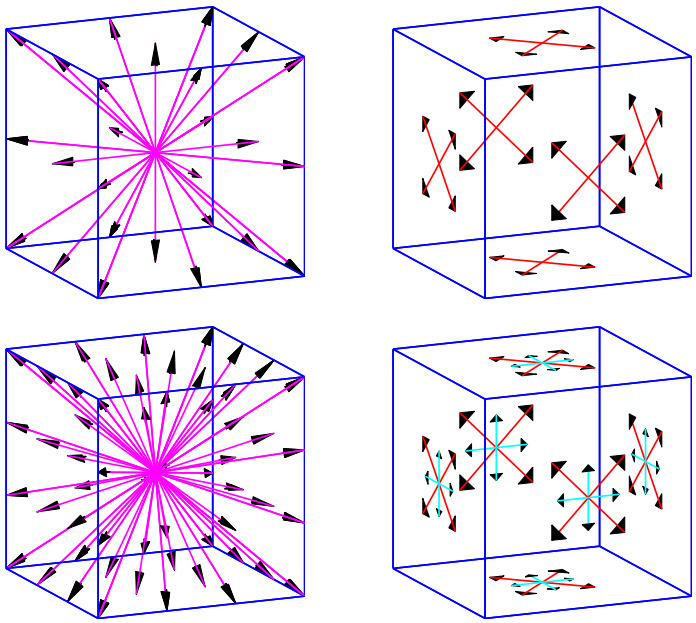

Figure 2. The hexahedral H-26-4 (top) and H-56-8 (bottom) elements for three-dimensional problems. The vectors in the left-hand side give the directions $\boldsymbol{\theta}_p$, and the vectors on the faces in the right-hand side describe the coefficients c_p and the directions $\boldsymbol{\phi}_p$.

2.3. Domain decomposition and regularization

The elements Ω_e are divided into n^d subdomains and the set of elements belonging to the dth subdomain is denoted by E^d. Then, the closure of the dth subdomain is given by

$$\bar{\Omega}^d = \bigcup_{e \in E^d} \bar{\Omega}_e. \tag{15}$$

In subdomains that do not touch the absorbing boundary Σ_2, a subdomain problem defined by the variational formulation (5) can have a local resonance frequency leading to an ill-posed problem. To avoid associated numerical difficulties, the regularization described in [10, 11] is adopted. More specifically, a regularization term is added on the subdomain boundaries as follows. For each subdomain, a sign s^d is chosen in such a way that two subdomains with a common edge/face have opposite signs if possible. For regular mesh partitions, this results in a checkerboard pattern for s^d. A constraint for s^d is that if Ω^d has an absorbing boundary condition on a part of its boundary then $s^d = 1$. Otherwise the subdomain problem could still be singular. A general algorithm for assigning the signs s^d can be found in [10]. After s^d is determined, an absorbing boundary condition of the form

$$\frac{\partial u}{\partial \boldsymbol{\nu}} = \gamma i s^{d,d'} k u \qquad \text{is introduced on} \quad \Gamma^{d,d'} = \partial\Omega^d \cap \partial\Omega^{d'}, \tag{16}$$

where $s^{d,d'}$ is an edge/face sign chosen to be $s^{d,d'} = s^d$ if $s^d \neq s^{d'}$, $s^{d,d'} = 0$ otherwise, and γ is a parameter satisfying $0 < \gamma \leq 1$.

Incorporating the additional subdomain boundary term (16) into the variational form (5) leads to the following modified bilinear form

$$\tilde{a}(u,v) = a(u,v) + \gamma \sum_{d=1}^{n^d} \sum_{\substack{d'=1 \\ d' \neq d}}^{n^d} \int_{\Gamma^{d,d'}} s^{d,d'} ikuvd\Gamma. \tag{17}$$

The bilinear forms a and $\tilde{a}$ coincide for functions that can be extended from $L^2(\widetilde{\Omega})$ to $H^1(\Omega)$ as the additional terms in (17) cancel each other on the opposite sides of the subdomain interfaces. In DEM, however, the solutions are usually slightly discontinuous over the element interfaces. Hence, the interface terms in (17) introduce some amount of regularization-induced error. The size of this error is controlled by the regularization parameter γ. One way to choose γ is to make the regularization error a fraction of the discretization error.

3. PRECONDITIONED ITERATIVE SOLVER

3.1. Interface problem

The discretization of the hybrid variational formulation (5) leads to a saddle point algebraic problem of the form

$$\begin{pmatrix} \mathbf{A} & \mathbf{B}^T \\ \mathbf{B} & \mathbf{0} \end{pmatrix} \begin{pmatrix} \mathbf{u} \\ \boldsymbol{\lambda} \end{pmatrix} = \begin{pmatrix} \mathbf{r} \\ \mathbf{0} \end{pmatrix}, \tag{18}$$

where the matrices $\mathbf{A}$, $\mathbf{B}^T$, and $\mathbf{B}$ correspond to the terms $a(u,v)$, $b(\lambda,v)$, and $b(\mu,u)$, respectively. The matrix $\mathbf{A}$ is block diagonal with each block corresponding to one element and of size equal to the number of waves in an element n_θ. Thus, the primal variable $\mathbf{u}$ can be efficiently eliminated from the saddle point problem to obtain the Schur complement system

$$\mathbf{F}\boldsymbol{\lambda} = \mathbf{B}\mathbf{A}^{-1}\mathbf{B}^T\boldsymbol{\lambda} = \mathbf{B}\mathbf{A}^{-1}\mathbf{r} = \mathbf{b}. \tag{19}$$

This system can be written in block form as follows

$$\mathbf{F}\boldsymbol{\lambda} = \begin{pmatrix} \mathbf{F}_{II} & \mathbf{F}_{IB} \\ \mathbf{F}_{BI} & \mathbf{F}_{BB} \end{pmatrix} \begin{pmatrix} \boldsymbol{\lambda}_I \\ \boldsymbol{\lambda}_B \end{pmatrix} = \begin{pmatrix} \mathbf{b}_I \\ \mathbf{b}_B \end{pmatrix}, \tag{20}$$

where the subscript I refers to the Lagrange multipliers in the interior of the subdomains and the subscript B refers to the Lagrange multipliers on the subdomain boundary interfaces.

The condensation of the interior Lagrange multipliers leads to yet another Schur complement system of the form

$$\mathbf{F}_S\boldsymbol{\lambda}_B = (\mathbf{F}_{BB} - \mathbf{F}_{BI}\mathbf{F}_{II}^{-1}\mathbf{F}_{IB})\boldsymbol{\lambda}_B = \mathbf{b}_B - \mathbf{F}_{BI}\mathbf{F}_{II}^{-1}\mathbf{b}_I = \mathbf{b}_S. \tag{21}$$

The above system of linear equations resembles that resulting from the FETI-DPH DD method for continuous polynomial discretizations. One main difference however is that here, the Lagrange multipliers are part of the discretization of the problem whereas for the FETI-DPH method they are artifacts of the decomposition of the problem into subdomains. Furthermore, in this case the interface Lagrange multipliers are edge/face based. One consequence is that in the proposed DD method, there are no corner Lagrange multipliers — that is, each Lagrange

multiplier is associated with two subdomains only. Once the interface Lagrange multipliers $\boldsymbol{\lambda}_B$ have been obtained from the solution of the above interface problem (21)), the interior ones are computed as follows $\boldsymbol{\lambda}_I = \mathbf{F}_{II}^{-1}(\mathbf{b}_I - \mathbf{F}_{IB}\boldsymbol{\lambda}_B)$ and the primal variable is obtained from $\mathbf{u} = \mathbf{A}^{-1}(\mathbf{r} - \mathbf{B}^T\boldsymbol{\lambda})$.

3.2. Local preconditioner

The objective is to solve problem (21) by a preconditioned GMRES algorithm.

First, a local preconditioner is constructed here with local subdomain operators in an additive manner. Using the restrictions of the bilinear forms a and b in (6) and (7), respectively, to a subdomain Ω^d can lead to a singular subdomain problem. In order to avoid this, an absorbing boundary condition is posed on the boundary $\Omega^d \setminus \Sigma$, where $\Sigma = \Sigma_1 \cup \Sigma_2$. Another reason to pose this boundary condition for the preconditioning problem is to let waves propagate out of the subdomain without much reflection on the boundary. The choice of these absorbing boundary conditions and its influence on the convergence of a nonoverlapping Schwarz method have been studied in [15, 19], for example. Here, the lowest order absorbing boundary condition is employed. Thus, the bilinear forms for subdomain Ω^d, $d = 1, \ldots, n^d$, that are proposed for constructing the local preconditioner are

$$a^d(u,v) = \int_{\Omega^d} (\nabla u \cdot \nabla v - k^2 uv) d\Omega - \int_{\Sigma_2 \cap \partial\Omega^d} M(u) v d\Gamma + \int_{\partial\Omega^d \setminus \Sigma} ikuv d\Gamma \tag{22}$$

and

$$b^d(\lambda, v) = \sum_{e \in E^d} \sum_{e'=1}^{e-1} \int_{\Gamma_{e,e'}} \lambda v|_{\Omega_{e'}} d\Gamma - \sum_{e=1}^{n_e} \sum_{\substack{e' \in E^d \\ e' < e}} \int_{\Gamma_{e,e'}} \lambda v|_{\Omega_e} d\Gamma \tag{23}$$

on $\mathcal{V}_{n_\theta}^d \times \mathcal{V}_{n_\theta}^d$ and $\mathcal{W}_{n_\lambda}^d \times \mathcal{V}_{n_\theta}^d$, respectively. Here, $\mathcal{V}_{n_\theta}^d$ and $\mathcal{W}_{n_\lambda}^d$ are subspaces of $\mathcal{V}_{n_\theta}$ and $\mathcal{W}_{n_\lambda}$, respectively, with their support in $\bar{\Omega}^d$. In the same way as the reduced problem (21) is constructed from the saddle point problem (18), the preconditioner in each subdomain is next reduced to a local operator acting on the interface Lagrange multipliers. First, with the above subdomain bilinear forms, a saddle point matrix

$$\begin{pmatrix} \mathbf{A}^d & \left(\mathbf{B}^d\right)^T \\ \mathbf{B}^d & \mathbf{0} \end{pmatrix} \tag{24}$$

is defined. Next, the primal variable is condensed out as in Section 3.1 to obtain a Schur complement matrix that can be written in block form as

$$\mathbf{F}^d = \mathbf{B}^d \left(\mathbf{A}^d\right)^{-1} \left(\mathbf{B}^d\right)^T = \begin{pmatrix} \mathbf{F}_{II}^d & \mathbf{F}_{IB}^d \\ \mathbf{F}_{BI}^d & \mathbf{F}_{BB}^d \end{pmatrix}, \tag{25}$$

and therefore is analogous to (20). Finally, the condensation of the interior Lagrange multipliers leads to the Schur complement matrix

$$\mathbf{F}_S^d = \mathbf{F}_{BB}^d - \mathbf{F}_{BI}^d \left(\mathbf{F}_{II}^d\right)^{-1} \mathbf{F}_{IB}^d. \tag{26}$$

The matrix $\mathbf{F}_S^d$ acts on the Lagrange multipliers associated with the subdomain boundary $\partial\Omega^d$. Let the restriction matrix $\mathbf{R}^d$ pick these Lagrange multipliers among all interface Lagrange multipliers.

Next, an additive local preconditioner is constructed based on the subdomain matrices $\mathbf{F}_S^d$. The action of this preconditioner is given by the multiplication by the matrix

$$\mathbf{C} = \sum_{d=1}^{n^d} \left(\mathbf{R}^d\right)^T \left(\mathbf{F}_S^d\right)^{-1} \mathbf{R}^d. \tag{27}$$

An efficient way to perform the multiplication $\mathbf{y} = \left(\mathbf{F}_S^d\right)^{-1} \mathbf{x}$ is to solve the system of linear equations

$$\begin{pmatrix} \mathbf{F}_{II}^d & \mathbf{F}_{IB}^d \\ \mathbf{F}_{BI}^d & \mathbf{F}_{BB}^d \end{pmatrix} \begin{pmatrix} \mathbf{z} \\ \mathbf{y} \end{pmatrix} = \begin{pmatrix} \mathbf{0} \\ \mathbf{x} \end{pmatrix} \tag{28}$$

using a sparse **LU** decomposition.

One can observe that the preconditioner described above has the matrix form of a primal Neumann-Neumann type of substructuring preconditioner [24] but applied to Lagrange multiplier degrees of freedom. However, the subdomain problems solved here are based on the hybrid variational formulation with a Robin boundary condition.

3.3. Coarse space projection

Next, following the idea of the two-level FETI method [12], a coarse space is formed and the system (21) is solved on its orthogonal complement. As it will be shown at the end of this section, this amounts to constructing a global preconditioner for problem (21).

Let the columns of a matrix $\mathbf{Q}$ span the coarse space. The construction of $\mathbf{Q}$ is described in Section 3.4. A projector onto the orthogonal complement of $\mathbf{Q}$ is defined as

$$\mathbf{P} = \mathbf{I} - \mathbf{Q}(\mathbf{Q}^T\mathbf{F}_S\mathbf{Q})^{-1}\mathbf{Q}^T\mathbf{F}_S. \tag{29}$$

Then it can be shown that the solution of (21) has the form

$$\boldsymbol{\lambda}_B = \boldsymbol{\lambda}_B^0 + \mathbf{P}\boldsymbol{\lambda}_B^1, \tag{30}$$

where $\boldsymbol{\lambda}_B^0 = \mathbf{Q}(\mathbf{Q}^T\mathbf{F}_S\mathbf{Q})^{-1}\mathbf{Q}^T\mathbf{b}_S$ and $\boldsymbol{\lambda}_B^1$ satisfies the system

$$\mathbf{P}^T\mathbf{F}_S\boldsymbol{\lambda}_B^1 = \mathbf{P}^T\mathbf{b}_S, \tag{31}$$

where $\mathbf{P}^T = \mathbf{I} - \mathbf{F}_S\mathbf{Q}(\mathbf{Q}^T\mathbf{F}_S\mathbf{Q})^{-1}\mathbf{Q}^T$.

Hence, the left preconditioned system reads

$$\mathbf{P}\mathbf{C}\mathbf{P}^T\mathbf{F}_S\boldsymbol{\lambda}_B^1 = \mathbf{P}\mathbf{C}\mathbf{P}^T\mathbf{b}_S. \tag{32}$$

Due to the identity $\mathbf{P}^T\mathbf{F}_S = \mathbf{F}_S\mathbf{P}$, the system (32) is equivalent to

$$\mathbf{P}\mathbf{C}\mathbf{F}_S\boldsymbol{\lambda}_B^1 = \mathbf{P}\mathbf{C}\mathbf{P}^T\mathbf{b}_S \tag{33}$$

when $\boldsymbol{\lambda}_B^1$ is in the range of $\mathbf{P}$. It is sufficient to have the solution only in this range as $\boldsymbol{\lambda}_B^1$ is multiplied by $\mathbf{P}$ in (30). The system (33) does not have a multiplication by $\mathbf{P}^T$ in the left-hand side and, thus, it is computationally less expensive in the iterative solution.

3.4. Coarse space construction

Following the FETI-H and FETI-DPH approaches presented in [10] and [7], respectively, the coarse space is constructed using plane waves. A rationale for this choice is as follows. The solution of the Helmholtz equation can be decomposed into plane waves and evanescent waves. The plane waves can travel far while the evanescent waves are more local as they decay with distance. The aim of the coarse space is to remove the components of the error that are non local — in this case, the plane waves — because iterative methods are usually more effective at correcting the local components of the error. The Lagrange multiplier λ in (5) gives the normal derivative of the solution u on edges/faces. Thus, by removing a sufficiently rich set of normal derivatives of plane waves from the error, its remaining components become local and effectively addressed by a locally preconditioned iterative method.

Given the motivation outlined above, the coarse space vectors are formed as the best representation of the normal derivatives of plane waves in the space of the Lagrange multipliers on the interfaces between subdomains. Specifically, a set of n_q plane waves is associated to each nonempty interface $\Gamma^{d,d'}$ between the subdomains Ω^d and $\Omega^{d'}$. (It can be expected that n_q will influence both the numerical scalability and computational cost of the resulting DD based iterative solver). With n_Γ nonempty interfaces, the number of vectors obtained this way is $n_q n_\Gamma$. For two-dimensional problems, a natural choice for the directions of the plane waves is given by $\boldsymbol{\theta}_p$ in (10) where n_θ is replaced by n_q. Similarly for three-dimensional problems, the directions $\boldsymbol{\theta}_p$ can be defined for $n_q = 8$, 26, 56, and 98 by (11) with $n_t = 1$, 2, 3, and 4, respectively. Let μ_j be the jth basis function of $\mathcal{W}_{n_\lambda}$ living on the interfaces between the subdomains and Γ^l be the lth nonempty interface $\Gamma^{d,d'}$. Then, the columns of $\mathbf{Q}$ are given by the best L^2 approximations

$$\mathbf{Q}_{(l-1)n_q+p} = \underset{\mathbf{q}}{\operatorname{argmin}} \left\| \frac{\partial}{\partial \boldsymbol{\nu}} \left(e^{ik\boldsymbol{\theta}_p^T \mathbf{x}} \right) - \sum_j q_j \mu_j \right\|_{0,\Gamma^l} \tag{34}$$

together with setting the components $\mathbf{Q}_{j,(l-1)n_q+p}$, $p = 1, \ldots, n_q$, to zero if the jth basis function μ_j is zero on Γ^l. Hence, the matrix $\mathbf{Q}$ can be computed by solving the system of linear equations

$$\mathbf{M}\mathbf{Q} = \mathbf{E}, \tag{35}$$

where the matrices $\mathbf{M}$ and $\mathbf{E}$ are defined by

$$\mathbf{M}_{j,n} = \int_\Gamma \mu_j \mu_n \, d\Gamma \qquad \text{and} \qquad \mathbf{E}_{j,(l-1)n_q+p} = \int_{\Gamma^l} \mu_j \frac{\partial}{\partial \boldsymbol{\nu}} \left(e^{ik\boldsymbol{\theta}_p^T \mathbf{x}} \right) d\Gamma, \tag{36}$$

where $\Gamma = \cup_l \Gamma^l$. After a permutation of rows and columns grouping together the Lagrange multipliers associated to the same edge/face of an element, the mass matrix $\mathbf{M}$ becomes diagonal. Hence, the solution of (35) is computationally inexpensive as the components of $\mathbf{Q}$ can be solved one edge/face at a time.

When an interface Γ^l is formed only by a few edges/faces, the number of Lagrange multipliers associated to it can be smaller than the number of plane waves n_q used to construct the coarse space. In this case, the Lagrange multiplier bases on Γ^l are included directly in the coarse space. This is accomplished by setting for $p = 1, \ldots, n_q$ the column $\mathbf{Q}_{(l-1)n_q+p}$ to zero except for the jth element of this column which is set to one if the Lagrange multiplier basis μ_j is the pth nonzero basis on Γ^l.

For the projector $\mathbf{P}$ in (29) to be well defined, the columns of $\mathbf{Q}$ must be linearly independent. Often $\mathbf{Q}$ has columns which are linearly dependent or very close to that. A larger number of directions n_q makes this more likely. For this reason the columns of $\mathbf{Q}$ are always orthogonalized. A column is removed from $\mathbf{Q}$ if its norm is reduced by some given factor ϵ after its has been made orthogonal to all previous columns. This orthogonalization can be made computationally more affordable by observing that each column is local to one interface Γ^l. Thus, it is sufficient to orthogonalize a column only with the other columns associated to the same interface.

4. NUMERICAL RESULTS

The numerical examples considered here are designed for assessing the convergence behavior of the GMRES algorithm applied to the solution of the preconditioned system of linear equations (33). In particular, the effects of the wavenumber k, the number of subdomains n^d, and the size of the coarse space N_Q on the iteration count are studied. CPU times are not reported as all computations were performed using a non optimized MATLAB implementation of the proposed DD solver. For comparison, the performance of the FETI-DPH method [7] for continuous polynomial discretizations of the same problems using the same meshes and biquadratic or tricubic elements is also reported.

The absorbing boundary condition on Σ_2 in (1) is chosen to be $\frac{\partial u}{\partial \boldsymbol{\nu}} = iku$. The reported iteration counts are for reducing the norm of the initial residual by the factor 10^{-7} without any GMRES restart. The drop tolerance for (nearly) linearly dependent columns in the orthogonalization of $\mathbf{Q}$ is set to $\epsilon = 10^{-6}$.

4.1. Two-dimensional acoustic scattering problem

Here, problem (1) is considered in the context of a circular scatterer. The computational domain is chosen to be $\Omega = \{\mathbf{x} \in \mathbb{R}^2 \ : \ 1 < \|\mathbf{x}\| < 2\}$. The incident field in (1) is set to the plane wave $g = e^{ikx_1}$. The regularization parameter γ in (16) is chosen to be 0.1. With this value, the additional error due to the regularization is a small fraction of the discretization error. The 24×2 domain decomposition chosen for this problem and its exact solution are shown in Figure 3.

Tables I and III report the performance of the proposed DD based iterative solver obtained using the Q-8-2 and Q-16-4 DGM elements, respectively, for different wavenumbers k and different domain decompositions. In these tables, N_Q does not include the columns of $\mathbf{Q}$ that are removed because of detected near linear dependence. Table II reports the performance results of the FETI-DPH method [7] for the continuous biquadratic finite element discretization of the same problem using the same meshes. In all tables, N denotes the size of the interface problem (33) or the corresponding system in the FETI-DPH method for continuous discretizations, and the columns "mesh" and n^d report the number of elements and number of subdomains, respectively, in the angular and radial directions. For the DGM discretizations, the errors reported in these tables (and in any other similar table in the remainder of this paper) are the relative errors of the averaged solution at the nodal points using the Euclidian norm.

For comparable sizes of the coarse spaces, the iteration counts of the proposed DD solver

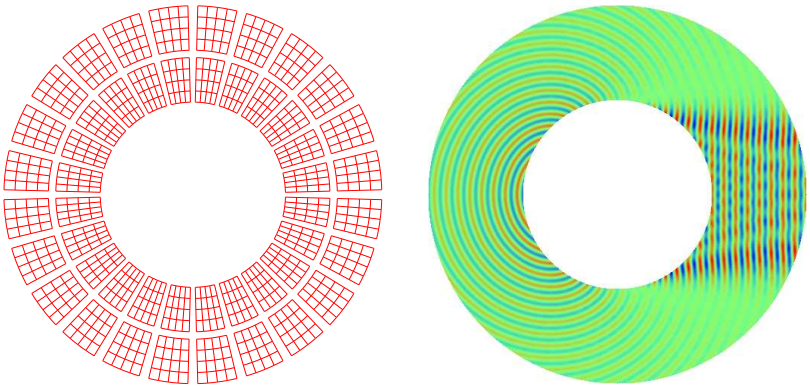

Figure 3. Circular scatterer: 24×2 domain decomposition for a 96×8 mesh and real part of the exact solution for $k = 16\pi$.

Table I. Circular scatterer: performance results of the proposed DD solver for the discretizations by Q-8-2 DGM elements.

			n_q	4		8		16		
k	mesh	n^d	N	$N_{\mathbf{Q}}$	iter.	$N_{\mathbf{Q}}$	iter.	$N_{\mathbf{Q}}$	iter.	error
4π	96×8	12×1	192	43	15	83	9	192	NA	$1.29e{-3}$
4π	96×8	24×2	576	262	20	576	NA	576	NA	$1.29e{-3}$
8π	192×16	12×1	384	43	27	83	18	163	10	$1.29e{-3}$
8π	192×16	24×2	1152	262	74	526	27	1152	NA	$1.29e{-3}$
8π	192×16	48×4	2688	1292	31	2688	NA	2688	NA	$1.30e{-3}$
16π	384×32	12×1	768	43	38	83	32	163	22	$1.54e{-3}$
16π	384×32	24×2	2304	262	189	526	79	1038	29	$1.54e{-3}$
16π	384×32	48×4	5376	1292	230	2460	57	5376	NA	$1.54e{-3}$

Table II. Circular scatterer: performance results of the FETI-DPH method for standard biquadratic finite elements discretizations.

k	mesh	n^d	N	$N_{\mathbf{Q}}$	iter.	$N_{\mathbf{Q}}$	iter.	$N_{\mathbf{Q}}$	iter.	error
4π	96×8	12×1	204	48	21	88	8	126	5	$2.34e{-2}$
4π	96×8	24×2	984	320	12	560	6	632	5	$2.34e{-2}$
8π	192×16	12×1	374	66	57	106	33	186	13	$3.41e{-2}$
8π	192×16	24×2	1128	288	57	552	14	804	6	$3.41e{-2}$
8π	192×16	48×4	2448	1440	17	2248	8	2458	7	$3.41e{-2}$
16π	384×32	12×1	758	66	81	106	66	186	41	$6.08e{-2}$
16π	384×32	24×2	2280	288	177	552	65	1024	27	$6.08e{-2}$
16π	384×32	48×4	5136	1440	170	2752	34	4076	9	$6.08e{-2}$

for discretizations by the Q-8-2 and Q-16-4 elements and those of the FETI-DPH method for the standard continuous Galerkin discretizations are fairly similar. For the lower frequency

Table III. Circular scatterer: performance results of the proposed DD solver for the discretizations by Q-16-4 DGM elements.

			n_q	4		8		16		
k	mesh	n^d	N	$N_{\mathbf{Q}}$	iter.	$N_{\mathbf{Q}}$	iter.	$N_{\mathbf{Q}}$	iter.	error
8π	48×4	12×1	192	43	27	83	17	192	NA	$2.81e{-3}$
8π	48×4	24×2	576	262	70	576	NA	576	NA	$2.81e{-3}$
16π	96×8	12×1	384	43	37	83	32	163	22	$2.97e{-3}$
16π	96×8	24×2	1152	262	182	526	73	1152	NA	$2.97e{-3}$
16π	96×8	48×4	2688	1292	219	2688	NA	2688	NA	$2.98e{-3}$
32π	192×16	12×1	768	43	44	83	43	163	36	$3.35e{-3}$
32π	192×16	24×2	2304	262	366	526	233	1038	105	$3.35e{-3}$
32π	192×16	48×4	5376	1292	623	2460	265	5376	NA	$3.35e{-3}$

regime, say $k = 4\pi$, fast convergence is observed for both iterative methods even when the size of the coarse space is only a small fraction of the size of the interface problem. In the higher frequency regime and for a large number of subdomains, fast convergence requires for both DD methods that the size of the coarse space be a significant fraction of the size of the interface problem.

For the same mesh, discretization by the Q-8-2 element is shown to provide a solution that is more than one order of magnitude more accurate than that delivered by the standard biquadratic finite elements. Discretization by the Q-16-4 element is shown to deliver a solution that is one order of magnitude more accurate than that predicted by the standard biquadratic finite elements, even when the number of Q-16-4 elements is halved in each direction compared with the number of continuous biquadratic elements. These observations illustrate the superior accuracy of the plane wave based elements that was demonstrated in [9, 13].

4.2. Three-dimensional acoustic scattering problem

Here, problem (1) is considered again but for a scatterer that is a cylinder capped with two hemispheres. The length of the scatterer, including the caps, is 12, the radius of the cylinder and hemispheres is 1. The computational domain is an ellipsoid with a semi-major axis of length equal to 7 (x_3-direction) and semi-minor axes of length equal to 3. The incident field is set to $g = e^{i\mathbf{k}\cdot\mathbf{x}}$, where $\mathbf{k} = (0.2\ 0.6\ 1)k/\sqrt{1.4}$. The regularization parameter γ (16) is set to 0.01. Two meshes with 1944 and 15552 elements are generated. The finer mesh is obtained by dividing each hexahedral element of the coarser mesh into eight smaller hexahedral elements. A cross cut of the fine mesh is shown in Figure 4. A domain decomposition of this mesh into 81 subdomains is displayed in Figure 5 and the solution for $k = 4\pi$ is graphically depicted in Figure 6. Table IV gathers various statistics about the size of the discretized problems.

Tables V and VII report the performance results obtained for the discretizations by the H-26-4 and H-56-8 elements, respectively. The wavenumber k is varied from π to 8π making the scatterer 6 to 48 wavelengths long. Two meshes are used in the numerical studies and the number of subdomains is varied from 11 to 164. For the mesh with 15552 elements decomposed into 159 subdomains, the coarse problem becomes too large to fit in memory for $n_q = 98$ (see Table VII). Table VI reports the performance results for the same physical problem but

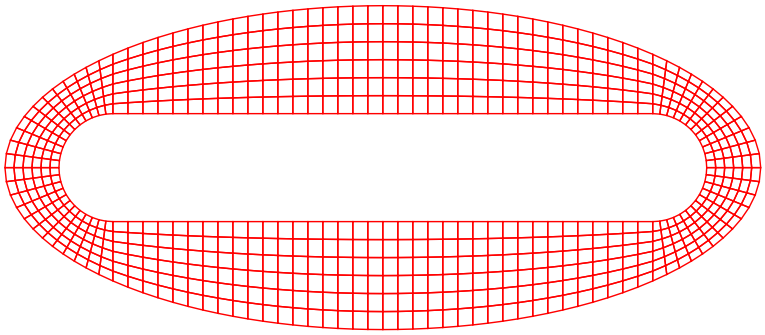

Figure 4. Capped cylindrical scatterer: cross cut in the (x_1, x_3) plane of the three-dimensional mesh with 15552 elements.

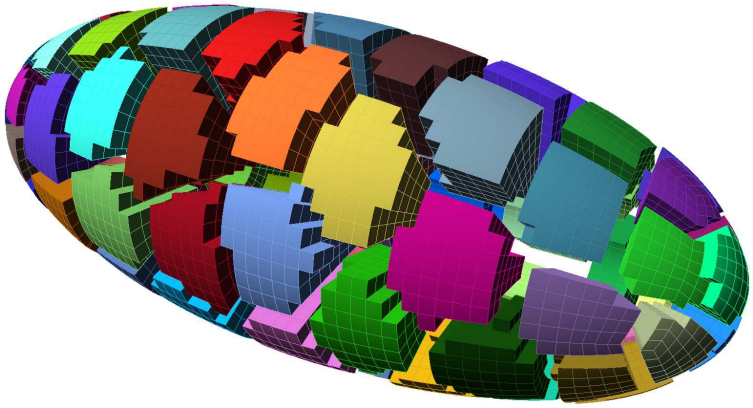

Figure 5. Capped cylindrical scatterer: decomposition of the computational domain in 81 subdomains.

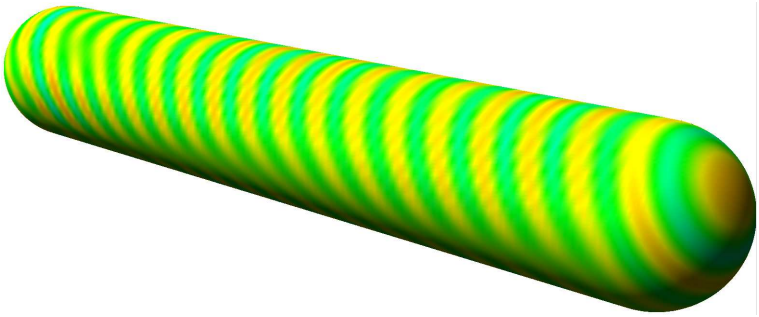

Figure 6. Capped cylindrical scatterer: numerical solution for $k = 4\pi$.

discretized by tricubic finite elements and solved by the FETI-DPH DD method equipped with the local Dirichlet preconditioner [7]. For this problem, all considered discretizations lead to the relative errors that are less than 10 percent [22]. For the same mesh, the standard tricubic finite

Table IV. Capped cylindrical scatterer: number of primal and Lagrange multiplier unknowns in the discretized problems.

	H-26-4		H-56-8		tricubic
elem.	primal	Lagrange multiplier	primal	Lagrange multiplier	primal
1944	50544	20736	108864	41472	58340
15552	404352	176256	870912	352512	443270

elements and the H-26-4 DGM elements are expected to deliver the same accuracy whereas the H-56-8 DGM element is expected to deliver a superior accuracy.

Table V. Capped cylindrical scatterer: performance results of the proposed DD solver for the discretizations by H-26-4 DGM elements.

			n_q	8		26		56		98	
k	elem.	n^d	N	$N_{\mathbf{Q}}$	iter.	$N_{\mathbf{Q}}$	iter.	$N_{\mathbf{Q}}$	iter.	$N_{\mathbf{Q}}$	iter.
π	1944	11	2300	192	38	614	26	1339	17	2126	10
π	1944	20	3056	388	42	1163	29	2487	17	3039	7
π	1944	40	4360	785	50	2407	31	4195	13	4360	NA
π	1944	80	5928	1527	75	4553	40	5928	NA	5928	NA
π	1944	164	8916	4140	88	8676	28	8916	NA	8916	NA
2π	1944	11	2300	192	56	614	37	1340	22	2126	11
2π	1944	20	3056	388	69	1163	39	2492	20	3043	6
2π	1944	40	4360	785	85	2407	39	4196	15	4360	NA
2π	1944	80	5928	1527	132	4553	50	5928	NA	5928	NA
2π	1944	164	8916	4142	155	8676	30	8916	NA	8916	NA
2π	15552	11	9120	216	57	696	42	1512	30	2614	25
2π	15552	20	12748	428	69	1366	45	2988	28	5069	23
2π	15552	40	16916	858	80	2630	45	5693	32	9191	29
2π	15552	81	24908	1734	123	5324	61	11647	42	18383	33
2π	15552	159	36564	4657	232	13820	112	26843	56	34879	24
4π	15552	11	9120	216	87	696	67	1512	50	2622	41
4π	15552	20	12748	428	114	1366	81	2988	52	5110	38
4π	15552	40	16916	858	146	2630	91	5702	55	9310	36
4π	15552	81	24908	1734	216	5324	135	11669	67	18703	40
4π	15552	159	36564	4657	444	13827	176	26942	68	35069	30

From Table V, it follows that for $k = 2\pi$, both DD methods applied to their respective problems exhibit the same convergence behavior when the size of the coarse space N_Q is less than half the size of the interface problem N. In Table VI, it is found that discretization by the H-26-4 elements leads to two to three times smaller interface problems than discretization by the tricubic finite elements. For $k = \pi$ and $k = 2\pi$, the FETI-DPH converges in general more rapidly than the proposed DD iterative solver. For $k = 4\pi$, the proposed DD method

Table VI. Capped cylindrical scatterer: performance results of the FETI-DPH DD solver for the discretizations by the standard tricubic elements.

			n_q	8		26		56		98	
k	elem.	n^d	N	$N_{\mathbf{Q}}$	iter.	$N_{\mathbf{Q}}$	iter.	$N_{\mathbf{Q}}$	iter.	$N_{\mathbf{Q}}$	iter.
π	1944	11	5983	205	15	636	8	1132	6	1214	6
π	1944	20	8097	415	13	1237	6	1724	5	1828	5
π	1944	40	11896	850	12	2286	6	2804	5	2920	5
π	1944	80	16870	1629	14	3726	6	4232	6	4395	6
π	1944	164	27968	4081	11	7697	6	8076	6	8352	6
2π	1944	11	5983	205	48	645	22	1332	9	2124	6
2π	1944	20	8097	416	53	1290	20	2492	10	3222	6
2π	1944	40	11896	854	76	2610	19	4389	8	5032	7
2π	1944	80	16870	1654	107	4636	23	6645	12	7266	11
2π	1944	164	27968	4158	177	9980	31	11808	27	12152	24
2π	15552	11	22154	230	42	716	21	1499	13	2257	10
2π	15552	20	31279	453	58	1412	22	2776	11	3702	9
2π	15552	40	42244	911	71	2760	15	4819	7	5766	6
2π	15552	81	63504	1850	95	5536	13	8800	8	9824	7
2π	15552	159	97952	4791	137	13534	32	18440	27	19352	25
4π	15552	11	22154	230	74	716	54	1526	43	2650	29
4π	15552	20	31279	453	125	1424	85	2998	63	5053	36
4π	15552	40	42244	912	191	2839	100	5683	74	8998	31
4π	15552	81	63504	1851	344	5749	177	11336	99	16674	28
4π	15552	159	97952	4804	> 500	14792	348	27090	101	34202	69

converges faster than FETI-DPH when the number of subdomains is greater than 11 and the coarse space is based on less than 98 plane waves.

From Table VII, it follows that for $k = 4\pi$, the proposed DD method exhibits the same convergence behavior for both considered meshes when the size of the coarse space is significantly smaller than that of the interface problem. From Table V and Table VII, it follows that the iteration counts of the proposed DD method are similar when either the H-26-4 or H-56-8 DGM element is used. However, when the frequency is doubled from $k = 2\pi$ to $k = 4\pi$ (Table V) or from $k = 4\pi$ to $k = 8\pi$ (Table VII), the number of iterations for convergence of the proposed DD method is shown to significantly increase.

5. Conclusions

An iterative domain decomposition method for the solution of Helmholtz problems discretized by the discontinuous enrichment method (DEM) [9, 13, 22, 25, 23] is presented. DEM can be described as a discontinuous Galerkin method with plane wave shape functions for approximating locally the solution and Lagrange multipliers for ensuring its weak continuity across the element interfaces. The proposed DD method iterates on the Lagrange multiplier

Table VII. Capped cylindrical scatterer: performance results of the proposed DD solver for the discretizations by H-56-8 DGM elements.

			n_q	8		26		56		98	
k	elem.	n^d	N	$N_{\mathbf{Q}}$	iter.	$N_{\mathbf{Q}}$	iter.	$N_{\mathbf{Q}}$	iter.	$N_{\mathbf{Q}}$	iter.
2π	1944	11	4600	192	57	614	38	1332	23	2382	16
2π	1944	20	6112	388	67	1201	37	2592	21	4526	17
2π	1944	40	8720	789	85	2467	39	5289	19	8163	13
2π	1944	80	11856	1527	108	4786	42	9552	22	11823	9
2π	1944	164	17832	4259	143	11942	38	17615	12	17832	NA
4π	1944	11	4600	192	72	614	60	1332	54	2382	40
4π	1944	20	6112	388	95	1201	74	2592	54	4531	34
4π	1944	40	8720	789	127	2467	86	5289	55	8163	21
4π	1944	80	11856	1527	167	4786	112	9552	57	11823	13
4π	1944	164	17832	4259	389	11942	113	17616	17	17832	NA
4π	15552	11	18240	216	87	696	67	1512	51	2636	40
4π	15552	20	25496	428	117	1366	82	2976	54	5254	39
4π	15552	40	33832	858	148	2662	92	5858	52	9824	31
4π	15552	81	49816	1738	228	5377	139	11826	64	20321	40
4π	15552	159	73128	4661	> 500	14341	193	30294	69		
8π	15552	11	18240	216	152	696	135	1512	121	2536	108
8π	15552	20	25496	428	190	1366	170	2976	151	5254	132
8π	15552	40	33832	858	243	2662	206	5858	174	9830	145
8π	15552	81	49816	1738	408	5377	343	11826	284	20330	211
8π	15552	159	73128	4661	> 500	14341	> 500	30295	351		

unknowns using a preconditioned GMRES algorithm. Preconditioning is performed in two steps. First, a local preconditioner is applied at the subdomain level. Then, a global preconditioner is constructed by requiring that at each GMRES iteration the residual be orthogonal to a coarse space. For both two- and three-dimensional acoustic scattering problems, it is found that the convergence of the proposed DD solver is almost independent of the mesh size and the number of plane waves in an element and therefore is numerically scalable with respect to these parameters. In the low frequency regime, the iteration count required by the proposed DD method for convergence is found to be slightly higher than that of the well-established FETI-DPH DD method for higher-order (quadratic and cubic) continuous discretizations [7]. In the higher frequency regime, both DD methods exhibit similar iteration counts. However, as was observed in [9, 13, 22], the accuracy of the solution delivered by DEM is significantly higher than that delivered by the standard finite element method of comparable order of convergence.

REFERENCES

1. T. Airaksinen, E. Heikkola, A. Pennanen, and J. Toivanen, *An algebraic multigrid based shifted-Laplacian preconditioner for the Helmholtz equation*, J. Comput. Phys., 226 (2007), pp. 1196–1210.

2. A. Brandt and I. Livshits, *Wave-ray multigrid method for standing wave equations*, Electron. Trans. Numer. Anal., 6 (1997), pp. 162–181.
3. F. Brezzi and M. Fortin, *Mixed and hybrid finite element methods*, vol. 15 of Springer Series in Computational Mathematics, Springer-Verlag, New York, 1991.
4. O. Cessenat and B. Despres, *Application of an ultra weak variational formulation of elliptic PDEs to the two-dimensional Helmholtz problem*, SIAM J. Numer. Anal., 35 (1998), pp. 255–299.
5. H. C. Elman, O. G. Ernst, and D. P. O'Leary, *A multigrid method enhanced by Krylov subspace iteration for discrete Helmhotz equations*, SIAM J. Sci. Comput., 23 (2001), pp. 1291–1315.
6. Y. A. Erlangga, C. W. Oosterlee, and C. Vuik, *A novel multigrid based preconditioner for heterogeneous Helmholtz problems*, SIAM J. Sci. Comput., 27 (2006), pp. 1471–1492.
7. C. Farhat, P. Avery, R. Tezaur, and J. Li, *FETI-DPH: a dual-primal domain decomposition method for acoustic scattering*, J. Comput. Acoust., 13 (2005), pp. 499–524.
8. C. Farhat, I. Harari, and L. P. Franca, *The discontinuous enrichment method*, Comput. Methods Appl. Mech. Engrg., 190 (2001), pp. 6455–6479.
9. C. Farhat, I. Harari, and U. Hetmaniuk, *A discontinuous Galerkin method with Lagrange multipliers for the solution of Helmholtz problems in the mid-frequency regime*, Comput. Methods Appl. Mech. Engrg., 192 (2003), pp. 1389–1419.
10. C. Farhat, A. Macedo, and M. Lesoinne, *A two-level domain decomposition method for the iterative solution of high frequency exterior Helmholtz problems*, Numer. Math., 85 (2000), pp. 283–308.
11. C. Farhat, A. Macedo, M. Lesoinne, F.-X. Roux, F. Magoulés, and A. de La Bourdonnaie, *Two-level domain decomposition methods with Lagrange multipliers for the fast iterative solution of acoustic scattering problems*, Comput. Methods Appl. Mech. Engrg., 184 (2000), pp. 213–239.
12. C. Farhat and J. Mandel, *A two-level FETI method for static and dynamic plate problems - part I: An optimal iterative solver for biharmonic systems*, Comput. Methods Appl. Mech. Engrg., 155 (1998), pp. 129–152.
13. C. Farhat, R. Tezaur, and P. Weidemann-Goiran, *Higher-order extensions of a discontinuous Galerkin method for mid-frequency Helmholtz problems*, Internat. J. Numer. Methods Engrg., 61 (2004), pp. 1938–1956.
14. C. Farhat, P. Wiedemann-Goiran, and R. Tezaur, *A discontinuous Galerkin method with plane waves and Lagrange multipliers for the solution of short wave exterior Helmholtz problems on unstructured meshes*, Wave Motion, 39 (2004), pp. 307–317.
15. M. J. Gander, F. Magoulès, and F. Nataf, *Optimized Schwarz methods without overlap for the Helmholtz equation*, SIAM J. Sci. Comput., 24 (2002), pp. 38–60.
16. E. Heikkola, T. Rossi, and J. Toivanen, *A parallel fictitious domain method for the three-dimensional Helmholtz equation*, SIAM J. Sci. Comput., 24 (2003), pp. 1567–1588.
17. U. Hetmaniuk and C. Farhat, *A fictitious domain decomposition method for the solution of partially axisymmetric acoustic scattering problems. II. Neumann boundary conditions*, Internat. J. Numer. Methods Engrg., 58 (2003), pp. 63–81.
18. T. Huttunen, P. Monk, and J. P. Kaipio, *Computational aspects of the ultra-weak variational formulation*, J. Comput. Phys., 182 (2002), pp. 27–46.
19. F. Magoulès, F.-X. Roux, and S. Salmon, *Optimal discrete transmission conditions for a nonoverlapping domain decomposition method for the Helmholtz equation*, SIAM J. Sci. Comput., 25 (2004), pp. 1497–1515.
20. J. M. Melenk and I. Babuška, *The partition of unity finite element method: basic theory and applications*, Comput. Methods Appl. Mech. Engrg., 139 (1996), pp. 289–314.
21. P. Monk and D.-Q. Wang, *A least-squares method for the Helmholtz equation*, Comput. Methods Appl. Mech. Engrg., 175 (1999), pp. 121–136.
22. R. Tezaur and C. Farhat, *Three-dimensional discontinuous Galerkin elements with plane waves and Lagrange multipliers for the solution of mid-frequency Helmholtz problems*, Internat. J. Numer. Methods Engrg., 66 (2006), pp. 796–815.
23. R. Tezaur, L. Zhang, and C. Farhat, *A discontinuous enrichment method for capturing evanescent waves in multiscale fluid and fluid/solid problems*, Comput. Methods Appl. Mech. Engrg., 197 (2008), pp. 1680–1698.
24. A. Toselli and O. Widlund, *Domain decomposition methods—algorithms and theory*, vol. 34 of Springer Series in Computational Mathematics, Springer-Verlag, Berlin, 2005.
25. L. Zhang, R. Tezaur, and C. Farhat, *The discontinuous enrichment method for elastic wave propagation in the medium-frequency regime*, Internat. J. Numer. Methods Engrg., 66 (2006), pp. 2086–2114.